Magnetization distribution in paramagnetic CoO: a polarized neutron diffraction study

2003 J. Phys.: Condens. Matter 15 3433

(http://iopscience.iop.org/0953-8984/15/20/306)

INSTITUTE OF PHYSICS PUBLISHING JOURNAL OF PHYSICS: CONDENSED MATTER

J. Phys.: Condens. Matter **15** (2003) 3433–3443 PII: S0953-8984(03)60534-5

Magnetization distribution in paramagnetic CoO: a polarized neutron diffraction study

N Kernavanois[1,3,4], E Ressouche[2], P J Brown[1], J Y Henry[2] and E Lelièvre-Berna[1]

[1] Institut Laue-Langevin, BP 156, 38042 Grenoble Cedex 9, France
[2] CEA-Grenoble, Département de Recherche Fondamentale sur la Matière Condensée, SPSMS-MDN, 17 rue des Martyrs, 38054 Grenoble Cedex 9, France

Received 5 March 2003
Published 12 May 2003
Online at stacks.iop.org/JPhysCM/15/3433

Abstract

Unpolarized and polarized neutron diffraction by a single crystal have been used to study the magnetization distribution in the paramagnetic phase of cobalt oxide CoO. Highly accurate magnetic structure factors have been measured using the classical polarized beam method. A detailed description of the magnetization distribution is presented. The magnetization around the cobalt site has a radial distribution which is contracted by $\simeq$5% with respect to that of the free ion and a symmetry which approximates more closely to e_g than to the form t_{2g}^5/e_g^2 expected for the Co^{2+} $3d^7$ configuration. A significant magnetization, corresponding to some 8% of the total moment, is found at the oxygen site.

(Some figures in this article are in colour only in the electronic version)

1. Introduction

The monoxides of the 3d transition metals MnO, FeO, CoO, and NiO form an interesting class of materials. Because of their apparently simple crystal and magnetic structures, they have been chosen as test samples for band theory models, and their electronic properties have been debated for a long time [1]. For example, their insulating behaviour remains unexplained, and more particularly this behaviour is in contradiction with simple models in which the oxygen p states are fully occupied, the metal s states are empty, and the metal d states are partially occupied. This failure is ascribed to a strong correlation between the 3d electrons, and two different explanations have been proposed: the Mott-insulator concept [2] and band calculations based on the local spin density approximation which take into account the antiferromagnetic order [3]. The orbital moment plays a key role in this latter approach, and as a result intensive experimental efforts have been made to determine its value [4–6].

[3] Author to whom any correspondence should be addressed.
[4] Previous address: European Synchrotron Radiation Facility, BP 220, 38043 Grenoble, France.

On the other hand, the electron distribution is a fundamental quantity which defines all the ground-state properties of a many-electron system [7]. An accurate determination of this quantity is thus also valuable for a better understanding of this class of materials. Recently, an experimental determination of the charge density in the unit cell of CoO has been undertaken using γ-ray diffraction [8]; it suggests that there is considerable redistribution of electrons upon magnetic ordering. With these data, the Co–O interaction has been identified as purely ionic, a character that is difficult to reconcile with the commonly assumed features of super-exchange.

Complementary information about the spatial extent of the unpaired electrons can also be obtained from neutron diffraction. The magnetic form factor can be derived from unpolarized neutron diffraction measurements of the intensities of magnetic Bragg peaks. This however requires a perfect knowledge of the magnetic structure, and huge difficulties are generally encountered in the derivation of the form factor due to uncertainties in the data treatment (extinction effects, Debye–Waller factor correction, ...). The form factor of cobalt in CoO was determined using this technique three decades ago [9], but owing to the large experimental uncertainties and the fact that the crystal and magnetic structures assumed were not the true ones [4], the conclusions drawn at this time cannot be considered to be definitive.

Much more precise measurements of the magnetic form factor can be made using polarized neutrons, with the help of the classical polarized beam method [10]. We have applied this technique to investigate the paramagnetic phase of CoO, and the purpose of this paper is to present a detailed analysis of the magnetization distribution obtained. Section 2 of the paper gives a brief presentation of the techniques used and the characterization of the sample. Section 3 presents the results of the preliminary nuclear structure refinement, using unpolarized neutrons. This step is of prime importance for the proper determination of the magnetization distribution described in section 4, where all our results are discussed and compared to previously established features of cobalt oxide. Finally, conclusions are drawn in section 5.

2. Experimental technique and sample characterization

The classical polarized neutron technique can be applied to single crystals which are magnetized by an external field. It consists in measuring the ratio, called the flipping ratio, between the intensities I^+ and I^- of a Bragg reflection, for an incident polarization of the neutron beam parallel (I^+) and antiparallel (I^-) to the applied field direction. This technique takes advantage of an interference term in the cross-section between the magnetic and nuclear amplitudes (provided that they occur at the same point in the reciprocal space), and is therefore well adapted to the study of ferromagnetic, ferrimagnetic, and paramagnetic systems. Its sensitivity to small magnetic contributions is much larger than that of the conventional unpolarized beam method. Further details of this technique can be found in [10]. As mentioned above, this method cannot be applied to the antiferromagnetic phase of CoO (since nuclear and magnetic scattering do not occur at the same positions in the reciprocal space), but can be used in the paramagnetic state, with an external magnetic field strong enough to induce significant polarization of the magnetization distribution.

Paramagnetic CoO has the NaCl-type crystal structure (space group $Fm3m$, cell parameter $a = 4.261$ Å at 300 K). In this structure, the cobalt atoms occupy the 4a sites (0, 0, 0), whereas the oxygen atoms are located at the 4b positions (1/2, 1/2, 1/2). The antiferromagnetic transition is accompanied by a cubic-to-monoclinic crystallographic distortion (space group $C2/m$ with Co at position 2a (0, 0, 0) and O at 2d (0, 1/2, 1/2)) [4]. All the different measurements described in this paper were performed on the same single crystal, grown using the Verneuil method, cut with a cubic shape (dimensions $\simeq 3 \times 3 \times 3$ mm^3), with two (001) and four (110) faces. The induced magnetic moments at $T = 300$ K under applied fields of

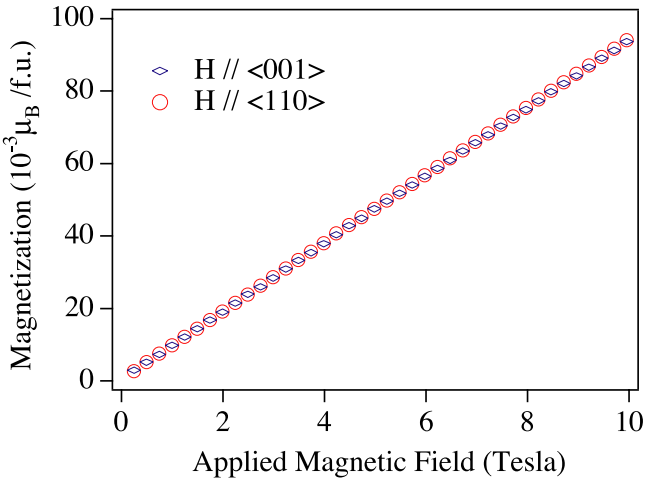

Figure 1. Magnetization curves at $T = 300$ K measured in CoO with an applied field along [001] and [110].

4.6 and 9.6 T (conditions used for the polarized neutron experiments) have been checked using a magnetometer: they reach 0.0435(2) and 0.0908(2) μ_B/fu respectively. Furthermore, no anisotropy between the [001] and the [110] directions has been detected under these conditions (figure 1): this is of prime importance for the polarized neutron data treatment, which usually assumes that the magnetization is aligned with the external magnetic field.

3. Nuclear structure refinement

The classical polarized beam technique requires the nuclear structure factors to be known very precisely in order to deduce the magnetic structure factors from the flipping ratios. Therefore, an unpolarized neutron diffraction experiment is often necessary to characterize the sample (in particular the magnitude of the extinction effect), under the same conditions as in the polarized neutron experiment. This preliminary experiment was performed on the two-axis D23-CEA-CRG (Collaborating Research Group) diffractometer at the Institut Laue-Langevin (ILL), Grenoble, France. D23 is a double-monochromator thermal-neutron diffractometer with a lifting detector arm. It has been used in the unpolarized beam mode (set-up I), with a copper monochromator, and at a wavelength $\lambda = 1.28$ Å.

40 independent reflections were measured at $T = 300$ K up to $\sin\theta/\lambda = 0.6$ Å^{-1}. Experimental data were corrected for absorption (linear absorption coefficient $\mu = 0.16$ mm^{-1}), using the Cambridge Crystallography Subroutine Library [11]. A $\lambda/2$ correction was also applied and refined together with the structural parameters, leading to a contamination value of $3.1(3) \times 10^{-4}$. The structural parameters were adjusted using the program MXD [12], with nuclear scattering lengths taken as 0.2490×10^{-12} and 0.5803×10^{-12} cm for the cobalt and the oxygen atoms respectively. The refinement led to a crystallographic weighted residual factor[5] $R_w(F^2) = 1.11\%$. This refinement included a Becker–Coppens Lorentzian correction of the extinction [13] that turned out to be rather weak ($\simeq$15% for the most extinguished reflections), and led to an extinction coefficient g of 1240(70) rad^{-1}, corresponding to a

[5] $R_w(F^2) = \sqrt{\sum[(I_{obs} - I_{calc})/\sigma_{I_{obs}}]^2 / \sum[I_{obs}/\sigma_{I_{obs}}]^2}$ where I_{obs} and I_{calc} are the observed and calculated intensities respectively and $\sigma_{I_{obs}}$ is the standard deviation.

crystal mosaicity $\eta = 1/(2\sqrt{\pi}g) = 0.78(5)'$. Attempts to let the oxygen occupation number vary were made, and led to 1 within error bars. This parameter was thus fixed to this value in the final refinement presented here.

The refined mean square amplitudes of vibration at 300 K amount to $U_{Co} = 0.0050(2)$ Å^2 and $U_O = 0.0064(1)$ Å^2, in perfect agreement with the values reported in [8], ($U_{Co} = 0.005\,18(2)$ Å^2 and $U_O = 0.006\,45(11)$ Å^2). This strongly supports the validity of both the Debye–Waller and the extinction corrections applied during the treatment of the polarized neutron data.

4. Magnetization distribution

Two different polarized neutron experiments have been performed. In the first, the D23 diffractometer was used in its polarized beam mode (set-up II); a Heusler alloy monochromator provided a polarized beam with a wavelength $\lambda = 1.32$ Å (polarization of the incident beam $P_+ = 0.94(1)$, $P_- = -0.94(1)$). The applied field was $H = 4.6$ T. In the second experiment, carried out on the two-axis diffractometer D3 at ILL, a much higher field ($H = 9.6$ T) was used; the polarized neutron beam of wavelength $\lambda = 0.85$ Å with $P_+ = 0.93(1)$, $P_- = -0.93(1)$ was again provided by a Heusler alloy monochromator.

These two polarized neutron experiments were carried out at $T = 300$ K under a magnetic field applied along the $\boldsymbol{c}$-axis. On D23, the flipping ratios $R = I^+/I^-$ were collected for 24 different Bragg reflections up to $\sin\theta/\lambda = 0.47$ Å^{-1}. On D3, 135 different Bragg reflections were collected up to $\sin\theta/\lambda = 0.94$ Å^{-1}. The data were corrected for extinction using the coefficient g refined from the previous unpolarized experiment. After symmetry averaging and merging of the data, a set of 22 independent magnetic structure factors $F_M(\boldsymbol{Q})$ was obtained.

The $F_M(\boldsymbol{Q})$ are nothing but the Fourier components of the magnetization distribution. To recover the distribution in real space, one has to solve an inverse Fourier problem, and several methods can be used [14]. We have chosen a model-free analysis of the data (maximum entropy method), and a parametrized model refinement (form factor analysis); the results from both techniques are presented in the following sections.

4.1. Maximum entropy reconstructions

The maximum entropy technique (MaxEnt) gives the most probable magnetization distribution map compatible with the measured structure factors and their experimental uncertainties [15–17]. This method has been shown to give much more reliable results than conventional Fourier syntheses, by considerably reducing both noise and truncation effects [17].

From the 22 independent experimental magnetic structure factors and the value of the macroscopic magnetization 0.0908(2) μ_B/fu (which corresponds to $F_M(\boldsymbol{Q} = 0)$), the magnetization distribution in the unit cell has been divided into $64 \times 64 \times 64$ cells (pixels) and reconstructed using a conventional uniform (flat) prior density. Such a procedure is biased against the creation of any magnetic density in the unit cell. Figure 2 shows the reconstructed magnetization distribution in CoO projected along the $[01\bar{1}]$ axis. This reconstruction immediately reveals two features that deserve particular attention: the presence of a strong anisotropic peak at the Co position on the one hand, and a weaker but well pronounced signal at the oxygen position on the other hand.

In the paramagnetic phase of CoO (cubic phase), each cobalt ion is at the centre of an oxygen octahedron. In a perfect octahedral field, the five d orbitals are split into the t_{2g} (xy, xz, yz) orbitals oriented towards the octahedral faces, and the e_g ($x^2 - y^2, 3z^2 - r^2$) ones, pointing towards the ligands. The Co^{2+} configuration is $3d^7(t_{2g}^5/e_g^2)$, and so two of the

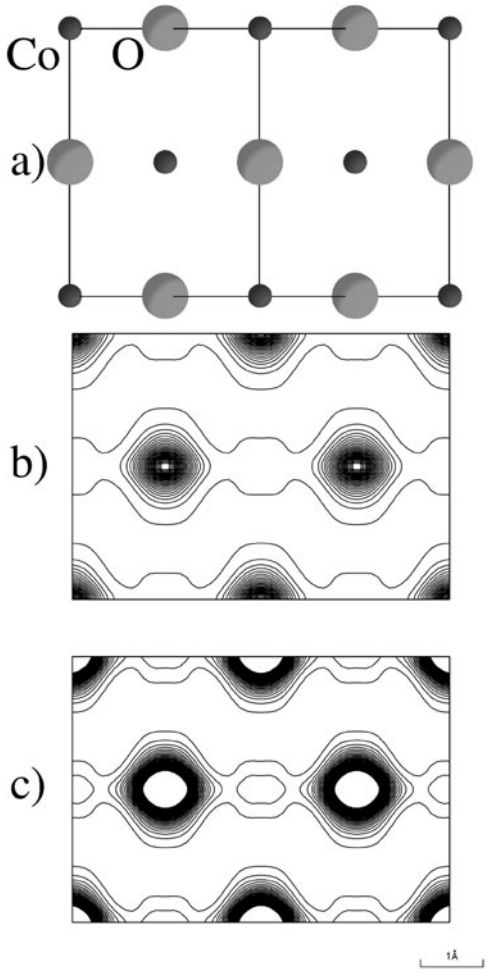

Figure 2. MaxEnt with a uniform prior. (a) Projection of the unit cell of CoO along the crystallographic $[01\bar{1}]$ axis. (b) Projection of the MaxEnt reconstructed magnetization distribution in CoO along the $[01\bar{1}]$ axis. The contour lines, drawn as solid lines, correspond to values from 0.0075 μ_B Å^{-2} up to 0.4575 μ_B Å^{-2} with a step of 0.015 μ_B Å^{-2} (high-level contours). (c) The same MaxEnt projection, with contour lines from 0.0075 μ_B Å^{-2} up to 0.1575 μ_B Å^{-2} with a step of 0.005 μ_B Å^{-2} (low-level contours).

unpaired electrons are expected to occupy e_g orbitals and the third a t_{2g} one. The fraction α of the unpaired electrons in e_g orbitals is therefore $\frac{2}{3} = 0.67$. Figure 3 shows some theoretical reconstructions of the magnetization distribution for different values of α: (a) a spherical distribution (corresponding to $\alpha = 0.40$); (b) the distribution for $\alpha = 0.67$; (c) the distribution with pure e_g symmetry ($\alpha = 1$); and (d) the distribution with pure t_{2g} symmetry ($\alpha = 0$). By simple comparison, the anisotropic peak reconstructed at the cobalt position using the flat prior hypothesis (figure 2) has a shape intermediate between that for $\alpha = 0.67$ (figure 3(b)) and that for $\alpha = 1$ (figure 3(c)), rather closer to the pure e_g case than to the expected configuration with $\alpha = \frac{2}{3}$.

To check whether the anisotropy on the cobalt atom or the magnetization on the oxygen site are artefacts of the MaxEnt technique, we repeated the procedure using different non-

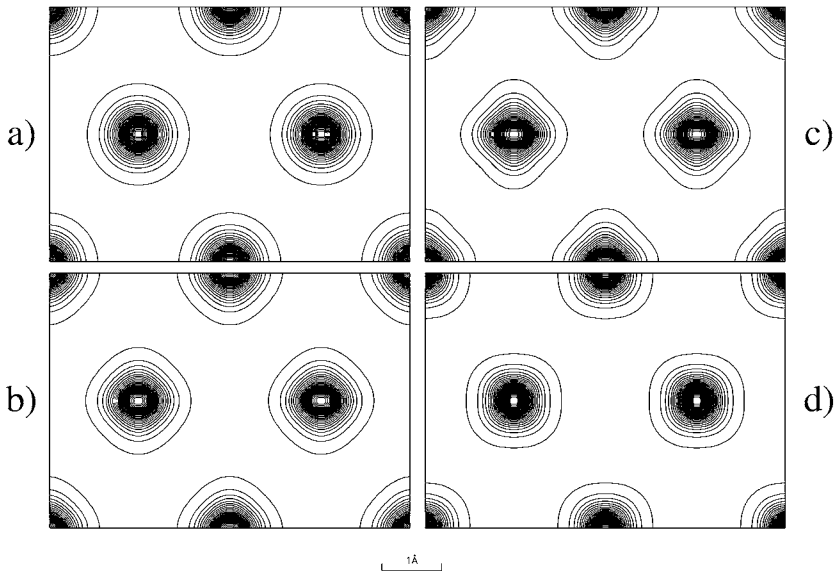

Figure 3. Projections of the magnetization distribution along $[01\bar{1}]$ for different models. (a) A spherical distribution ($\alpha = 0.40$); (b) the distribution expected for a Co^{2+} ion in a perfect octahedral field ($\alpha = 0.67$); (c) the pure e_g orbital ($\alpha = 1$); (d) the pure t_{2g} orbital ($\alpha = 0$).

uniform prior distributions [18]. In these reconstructions the bias against the creation of either magnetic density on oxygen sites or spurious asphericity of the Co density should be considerably enhanced as compared to that with the uniform prior strategy. To start with, all the magnetization in the crystal has been assumed to be spherically concentrated around the Co sites, with no magnetization of the oxygen atoms (model 1); this non-uniform prior corresponds to figure 3(a). In a second step, the model depicted in figure 3(b) ($\alpha = 0.67$) was used for the prior density, with again no density on the oxygen atom (model 2). Figure 4 shows the resulting projections of the two MaxEnt reconstructions along the $[01\bar{1}]$ axis (upper part), and the differences between the reconstructions and the reference model (lower part).

As can be seen immediately from figure 4, both the features of interest: the magnetization on the oxygen site and the asphericity of the Co distribution, survive the stringent test of non-uniform priors. Both reference models still leave a clear signal at the anion sites. Moreover, both reconstructions show added magnetization along the Co–O bonds, consistent with a depletion of the t_{2g} orbital in favour of the e_g one. The fact that these two features are independent of the prior density is a strong indication that they are real properties of the magnetization distribution which must be addressed in any theoretical treatment.

4.2. Form factor refinements

The magnetic structure factor can be expressed as the product of the total magnetic moment (spin + orbit) and the form factor as

$$F_M(\boldsymbol{Q}) = \sum_{j\ atoms} \mu_j f_j(\boldsymbol{Q}) \mathrm{e}^{\mathrm{i}\boldsymbol{Q}\cdot\boldsymbol{r}_j} \mathrm{e}^{-W_j} \tag{1}$$

where μ_j, $f_j(\boldsymbol{Q})$, $\boldsymbol{r_j}$, and e^{-W_j} are respectively the moment, the form factor, the position, and the Debye–Waller factor of atom j in the unit cell. $\boldsymbol{Q} = (hkl)$ is the scattering vector. Due

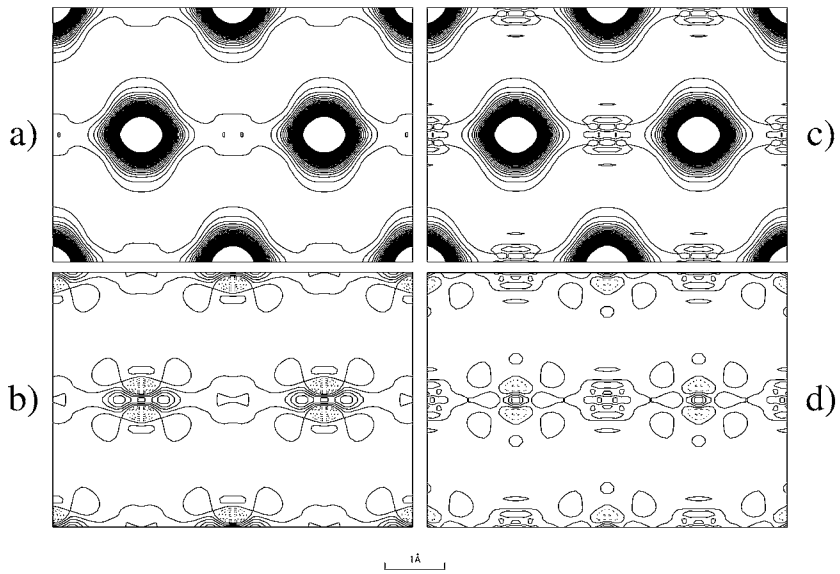

Figure 4. MaxEnt with non-uniform priors. Projections of the magnetization density along $[01\bar{1}]$. Upper part: MaxEnt reconstruction starting with model 1(a) and model 2(c) as the non-uniform prior. The contour lines correspond to values from 0.0075 μ_B Å^{-2} up to 0.1575 μ_B Å^{-2}, with a step of 0.005 μ_B Å^{-2}. Lower part: differences between reconstructions and models. The contour lines correspond to values from -0.0275 μ_B Å^{-2} up to 0.0275 μ_B Å^{-2}, with a step of 0.005 μ_B Å^{-2}. Dashed lines are negative contours.

to the special positions occupied by cobalt and oxygen atoms in CoO, the magnetic structure factor can be simply written as

$$F_M(\boldsymbol{Q}) = 4 \times (\mu_{\mathrm{Co}} f_{\mathrm{Co}}(\boldsymbol{Q}) \mathrm{e}^{-W_{\mathrm{Co}}} + (-1)^{h+k+l} \mu_{\mathrm{O}} f_{\mathrm{O}}(\boldsymbol{Q}) \mathrm{e}^{-W_{\mathrm{O}}}). \tag{2}$$

Assuming that both spin (S) and orbital (L) moments are present on the cobalt site,

$$\mu_{\mathrm{Co}} f_{\mathrm{Co}}(\boldsymbol{Q}) = \mu^S_{\mathrm{Co}} f^S_{\mathrm{Co}}(\boldsymbol{Q}) + \mu^L_{\mathrm{Co}} f^L_{\mathrm{Co}}(\boldsymbol{Q}). \tag{3}$$

As already seen, in a perfect octahedral field, the d orbitals are split into the t_{2g} and the e_g subsets. For an e_g and a t_{2g} electron, one has respectively

$$f^S_{\mathrm{e_g}}(\boldsymbol{Q}) = \langle j_0(\boldsymbol{Q}) \rangle + \tfrac{3}{2} A(\boldsymbol{Q}) \langle j_4(\boldsymbol{Q}) \rangle \tag{4}$$

and

$$f^S_{\mathrm{t_{2g}}}(\boldsymbol{Q}) = \langle j_0(\boldsymbol{Q}) \rangle - A(\boldsymbol{Q}) \langle j_4(\boldsymbol{Q}) \rangle \tag{5}$$

where the $\langle j_L(\boldsymbol{Q}) \rangle$ are the radial integrals (Bessel–Fourier transform of order L) of the radial density and $A(\boldsymbol{Q})$ depends only on the Miller indices (hkl) of $\boldsymbol{Q}$:

$$A(\boldsymbol{Q}) = \frac{h^4 + k^4 + l^4 - 3(h^2k^2 + h^2l^2 + k^2l^2)}{(h^2 + k^2 + l^2)^2}. \tag{6}$$

If we assume that a fraction α of the unpaired electrons are in the e_g orbitals, the remaining $(1 - \alpha)$ being in the t_{2g} orbitals, the spin contribution to the form factor can be written as

$$\mu^S_{\mathrm{Co}} f^S_{\mathrm{Co}}(\boldsymbol{Q}) = \mu^S_{\mathrm{Co}} (\langle j_0(\boldsymbol{Q}) \rangle + (\tfrac{5}{2}\alpha - 1) A(\boldsymbol{Q}) \langle j_4(\boldsymbol{Q}) \rangle). \tag{7}$$

In the dipolar approximation, the orbital contribution $\mu^L_{\mathrm{Co}} f^L_{\mathrm{Co}}(\boldsymbol{Q})$ is

$$\mu^L_{\mathrm{Co}} f^L_{\mathrm{Co}}(\boldsymbol{Q}) = \mu^L_{\mathrm{Co}} (\langle j_0(\boldsymbol{Q}) \rangle + \langle j_2(\boldsymbol{Q}) \rangle). \tag{8}$$

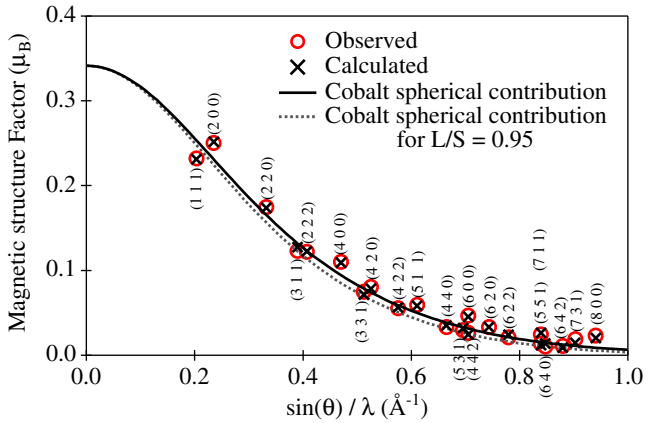

Figure 5. The result of the form factor refinement for CoO. The circles show observed magnetic structure factors (corresponding to four formula units). Crosses show the corresponding calculated values. The solid and dashed curves show the spherical contributions of cobalt atoms for different values of the L/S ratio.

As far as the oxygen is concerned, since its contribution is weak (as shown by the MaxEnt results), it can be approximated by its spherical (spin-only) part:

$$\mu_O f_O(\boldsymbol{Q}) = \mu_O \langle j_0(\boldsymbol{Q}) \rangle. \tag{9}$$

Inserting equations (7)–(9) into (2) gives an expression for the magnetic structure factor of CoO. We have used this expression in a least-squares procedure to derive μ^S_{Co}, μ^L_{Co}, μ_O, and α from our 22 independent experimental observations. The values of the radial integrals used are those tabulated in [19] for a free Co^{2+} ion. For the oxygen contribution, a radial integral $\langle j_0(\boldsymbol{Q}) \rangle$ has been calculated from the standard Slater exponent tabulated in [20] ($\zeta = 2.25$ au).

The result of this analysis is shown in figure 5. The parameters obtained are $\mu^S_{Co} = 0.045(2)\ \mu_B$, $\mu^L_{Co} = 0.041(1)\ \mu_B$, $\mu_O = 0.008(1)\ \mu_B$, and $\alpha = 0.83(4)$. The corresponding χ^2 is equal to 1.00.

The first point worthy of comment is the induced magnetization on the oxygen atom. This polarization, already shown by the MaxEnt reconstruction, is confirmed by this analysis. Although small, the result is unambiguous, since it is eight times larger than its standard deviation, and represents roughly 8% of the total magnetization. This contribution cannot be explained by chemical disorder, since our attempts to refine the oxygen occupation number led to 1 within roughly 2%. A similar effect has already been observed for other magnetized antiferromagnets, for example the garnet $Ca_3Fe_2Ge_3O_{12}$ [21], and the layered perovskite ruthenate $Ca_{1.5}Sr_{0.5}RuO_4$ [22]. It has been explained in terms of the covalent interaction inherent in the super-exchange mechanism which gives rise to the antiferromagnetic coupling. Three effects are expected in such a case:

(i) a reduction of the magnetic moment on the anion compared to its free-ion value due to a partial transfer to the ligands;
(ii) the appearance of an overlap density which creates a node between the magnetic ion and the ligand;
(iii) the appearance of magnetization on the ligand itself with the same sign (direction) as on the anion (covalent spin density).

In a simple antiferromagnet, the magnetizations on either side of the ligand have opposite signs and so the covalent spin density may be exactly cancelled. By contrast, in the paramagnetic

phase of an antiferromagnet, the magnetization transferred to the ligand is always in the direction of the applied field and so builds up rather than cancelling. In the garnet, the transfer to the ligand amounted to 14% and in the ruthenate to 20% of the total moment, which is roughly twice what is observed here.

The second point concerns the total magnetization: adding $\mu^S_{\rm Co}$, $\mu^L_{\rm Co}$, and $\mu_{\rm O}$ gives $\mu_{\rm tot} = 0.094(3)\ \mu_B$, which compares rather well with the $0.0908(2)\ \mu_B$/fu measured with the magnetometer under the same conditions. The total magnetization in the unit cell is thus well reproduced by the form factor analysis.

The asymmetry of the magnetization distribution also deserves comment. The refined value for the parameter $\alpha = 0.83(4)$ is quite surprising. The theoretical value for the cobalt configuration $3d^7$ (t^5_{2g}/e^2_g) is 0.67, and the value of 0.83(4) obtained looks too high. It should be noticed, however, that this result could be anticipated from the MaxEnt analysis since in all the reconstructions the shape of the magnetization around the cobalt ion is very close to that of an e_g orbital. In particular, even the reconstruction using $\alpha = 0.67$ in the non-uniform prior shows additional magnetization along the Co–O bonds as compared to the reference model. In [8], Jauch *et al* have estimated the number of unpaired electrons in the different d orbitals from a charge density determination using γ-ray diffraction: in the paramagnetic state they deduce that 3.6 electrons are unpaired, 1.8 in the e_g orbitals with the remaining 1.8 in t_{2g} orbitals. This repartition leads to $\alpha = 0.50$. In the ordered state, they claim that there is a considerable redistribution between the different orbitals: only 2.4 unpaired electrons remain, of which 1.5 are in e_g orbitals, giving $\alpha = 0.63$. Our present result is quite different, but is however in qualitative agreement with simple bond length considerations. The ionic radius of an O^{2-} ion with coordination number 6 being 1.40 Å [23], this leads, in a hard-sphere model of the face-centred cubic structure, to a radius of 0.73 Å for the cobalt ion. As the radius of Co^{2+} in a sixfold coordination and high-spin state (t^5_{2g}/e^2_g) is 0.745 Å [23], one could expect the stresses induced by this slightly smaller value to be relaxable by a partial change of the electronic state towards the low-spin state (pure e_g), the radius of which is smaller (0.65 Å).

Even more surprising and rather unrealistic are the refined values of $\mu^L_{\rm Co} = 0.041(1)\ \mu_B$ and $\mu^S_{\rm Co} = 0.045(2)\ \mu_B$, which would imply that half the moment on the cobalt site is due to orbital motion. From these values, the ratio $L/S = 2 \times \mu^L_{\rm Co}/\mu^S_{\rm Co} = 1.8(1)$ can be deduced. This value is twice as big as $L/S = 0.95$ reported from magnetic x-ray scattering studies [5]. Another determination of this ratio has been performed by Jauch *et al* [8], combining two different techniques. From powder neutron diffraction experiments, performed in the light of new synchrotron powder diffraction results that clearly establish a monoclinic crystal structure in the antiferromagnetic phase of CoO [4], these authors have found a magnetic moment of $3.98(6)\ \mu_B$ per cobalt ion. In their charge density determination by means of γ-ray diffraction already mentioned [8], the same group found that the number of unpaired electrons in the ordered state was 2.40(9). A simple difference between these two quantities (assuming that 2.40 unpaired electrons result in a $2.40\ \mu_B$ spin moment) leads to an orbital magnetic moment of $1.6\ \mu_B$, and as a consequence $L/S = 1.3(1)$, a value rather lower than what we have found. Figure 5 shows the spherical contributions to the form factor obtained with our set of parameters (solid line), and with $L/S = 0.95$ (dashed). It is clear that the experimental form factor that we have measured is more extended in reciprocal space (meaning that the corresponding orbitals are more contracted in direct space) than would be expected for a free Co^{2+} ion. A similar contraction has already been observed in the ordered phase from the unpolarized neutron determination of the form factor of cobalt in CoO [9]. Such an effect has also been found in NiO [24, 25], whereas for other transition metal compounds the use of free-atom form factors works rather well.

Table 1. Results of the two types of least-squares refinement. In the first the ratio L/S was fixed, while α, the spin moment on cobalt, the moment on oxygen, and κ varied. For the second type of refinement, α was fixed and L/S, the spin moment on the cobalt, the moment on the oxygen, and κ were allowed to vary. The χ^2 corresponding to each refinement is also indicated together with the expansion of the form factor corresponding to the deviation from 1 of the κ-parameter value expressed as a percentage. This expansion coefficient cannot be ascribed to the unquenched orbital magnetic moment which is already taken into account in the refinement (cf equation (3)).

L/S	μ^S_{Co}	μ_O	α	κ	χ^2	Expansion (%)
0.95 fixed	0.057(1)	0.008(1)	0.76(3)	0.94(1)	1.03	6
1.3 fixed	0.051(1)	0.008(1)	0.79(3)	0.97(1)	1.00	3
0.6(3)	0.064(8)	0.008(1)	0.50 fixed	0.90(4)	4.90	10
0.5(3)	0.066(7)	0.008(1)	0.63 fixed	0.89(3)	1.86	11

To shed some light on these two problems, some further analyses have been made. In order to compare our results with those obtained by Alperin in [24] we have introduced the adjustable parameter κ used by Alperin to explain the form factor of nickel in NiO in terms of form factor expansion. In equation (2) (which gives the cobalt scattering) $\boldsymbol{Q}$ has been replaced by $\kappa\boldsymbol{Q}$. Two types of least-squares refinement have then been carried out fixing either the ratio L/S or α. All the results are summarized in table 1. It is clear from these results that the effect of α (the fraction of electrons in e_g orbitals) on the goodness of fit (χ^2) is huge: it is impossible to obtain good agreement with our data with any value of α smaller than $\simeq$0.75. This is in complete contradiction with the charge density work. Fixing the L/S ratio gives much better fits in terms of χ^2, suggesting a 3–6% contraction of the 3d orbitals compared to the free ion. This contraction is in good agreement with that reported in [8] and from the previous unpolarized neutron determination of the form factor of cobalt in CoO [9]. In this latter work, the spherical component of the magnetic form factor of Co has been found to be expanded by between 15 and 17% compared to the spin-only free-ion curve. 11% of the expansion was attributed to the unquenched orbital magnetic moment [26], and the remaining 4–6% corresponds well with what has been observed in the present experiment (refinements with the ratio L/S fixed to 0.95 and 1.3 lead respectively to 6 and 3% expansion of the form factor).

5. Conclusions

In this work, we have presented a polarized neutron diffraction study of the magnetization distribution in a single crystal of CoO in the paramagnetic phase. From our experimental results, several points have been firmly established. We have observed a significant magnetic moment on the oxygen atoms, that represents roughly 8% of the total induced magnetization. Although such an effect is expected, and has already been observed in other compounds, it is the first time that it has been found in such a simple system as the transition metal monoxides. Our data also demonstrate a strong anisotropy of the cobalt form factor showing that the unpaired electron distribution has symmetry closer to e_g than to the t_{2g}^5/e_g^2 expected for the Co^{2+} $3d^7$ configuration. Last but not least, this experiment has confirmed the form factor expansion already observed in the antiferromagnetic phases of CoO and NiO. It has shown that this effect is real and cannot be wholly accounted for by either covalency, orbital scattering, or spin polarization effects. Since this form factor expansion, which has yet to be explained, has been observed in both the paramagnetic and the ordered states, it must be considered as an intrinsic property of Co^{2+} ions in CoO rather than a consequence of the antiferromagnetic ordering.

Acknowledgments

We would like to thank Dr R Ballou (Laboratoire Louis Néel, CNRS-Grenoble) for his help during the magnetometric measurements and Dr J Schweizer (CEA-Grenoble) for many fruitful and stimulating discussions.

References

[1] Cox P A 1992 *Transition Metal Oxides* (Oxford: Oxford University Press)
[2] Mott N F 1949 *Proc. Phys. Soc.* A **62** 416
[3] Terakura K, Williams A R, Oguchi T and Kübler J 1984 *Phys. Rev. Lett.* **52** 1830
[4] Rauch W, Reehuis M, Bleif H J and Kubanek F 2001 *Phys. Rev.* B **64** 052102
[5] Neubeck W, Vettier C, de Bergevin F, Yakhou F, Mannix D, Ranno L and Chatterji T 2001 *J. Phys. Chem. Solids* **62** 2173
[6] Vidal J P, Vidal-Valat G, Kurki-Suonio K and Kurki-Suonio R 2002 *Crystallogr. Rep.* **47** 391
[7] Hohenberg P and Kohn W 1964 *Phys. Rev.* **136** B864
[8] Rauch W and Reehuis M 2002 *Phys. Rev.* B **65** 125111
[9] Khan D C and Erickson R A 1970 *Phys. Rev.* B **1** 2243
[10] Nathans R, Pigott M T and Shull C G 1958 *J. Phys. Chem. Solids* **6** 38
[11] Brown J and Matthewman J 1993 Cambridge Crystallography Subroutine Library *Rutherford Appleton Laboratory Report* No 93-009
[12] Wolfers P 1990 *J. Appl. Crystallogr.* **23** 554
[13] Becker P J and Coppens P 1974 *Acta Crystallogr.* A **30** 129
[14] Brown P J 1993 *Int. J. Mod. Phys.* B **7** 3029
[15] Gull S F and Daniell G J 1978 *Nature* **272** 686
[16] Skilling J and Gull S F 1985 *Maximum Entropy and Bayesian Methods in Inverse Problems* ed C R Smith and W T Grandy Jr (Dordrecht: Reidel) p 83
[17] Papoular R J and Gillon B 1990 *Europhys. Lett.* **13** 429
[18] Zheludev A, Papoular R J, Ressouche E and Schweizer J 1995 *Acta Crystallogr.* A **51** 450
[19] Brown P J 1992 *International Tables for Crystallography* ed A J C Wilson (Dordrecht: Kluwer–Academic) p 391
[20] Hehre W J, Stewart R F and Pople J A 1969 *J. Chem. Phys.* **51** 2657
[21] Plakhty V P, Gukasov A G, Papoular R J and Smirnov O P 1999 *Europhys. Lett.,* **48** 233
[22] Gukasov A, Braden M, Papoular R J, Nakatsuji S and Maeno Y 2002 *Phys. Rev. Lett.* **89** 087202
[23] Shannon R D 1976 *Acta Crystallogr.* A **32** 751
[24] Alperin H A 1961 *Phys. Rev. Lett.* **6** 55
[25] Brown P J 2003 private communication
[26] Mahendra A and Khan D C 1971 *Phys. Rev.* B **4** 3901